Linear stability of nontrivial phase solutions of the cubic Nonlinear Schrödinger equation

Draft - August 1, 2005

Abstract

We study the two dimensional cubic Nonlinear Schrödinger (NLS) equation, which admits a large family of one-dimensional traveling wave solutions. All such bounded solutions may be written in a amplitude-phase decomposition. In the form we present, the phase of this solution is dependant on the spatial dimension of the one-dimensional wave-form. We first compute a linearization of the NLS equation around these exact solutions. This linearization is then used to study the linear stability of solutions having non-constant phase dependency, using a spectrally based method. We present numerical evidence which suggests that these solutions are unstable to perturbations that are transverse to the one-dimensional traveling wave. This transverse instability occurs in both elliptic and hyperbolic cases, and in the focusing and defocusing setting.

1 Introduction

The cubic Nonlinear Schrödinger (NLS) equation in two spatial dimensions is given by

$$i\psi_t + \alpha\psi_{xx} + \beta\psi_{yy} + |\psi|^2\psi = 0. \tag{1}$$

This equation admits a large family of one-dimensional traveling wave solutions. These solutions may be written in the form

$$\psi(x,t) = \phi(x)e^{i\lambda t + i\theta(x)}, \tag{2}$$

where $\phi(x)$ and $\theta(x)$ are real-valued functions, and ω is a real constant. Bounded solutions of the form (2) are possible if

$$\phi^2(x) = \alpha\left(-2k^2\,\mathrm{sn}^2(x,k) + B\right), \tag{3}$$

$$\theta(x) = c\int_0^x \phi^{-2}(\xi)d\xi, \tag{4}$$

$$\lambda = \frac{1}{2}\alpha(3B - 2(1+k^2)), \qquad \text{and} \tag{5}$$

$$c^2 = -\frac{\alpha^2}{2}B(B-2k^2)(B-2). \tag{6}$$

Here $k \in (0,1)$ is the elliptic modulus of the Jacobi elliptic sine function denoted by $\mathrm{sn}\,(x,k)$. Later we use the fact that $\mathrm{sn}\,(x,k)$ is periodic, with period given by $L = 4K$, with

$$K(k) = \int_0^{\pi/2}\left(1 - k^2\sin^2 x\right)^{-1/2}\,dx.$$

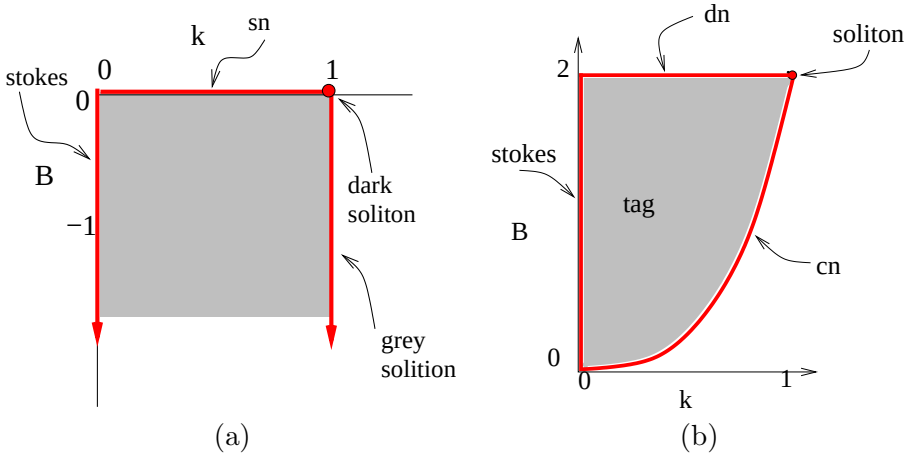

Figure 1: Admissible parameter space for defocusing (a) and focusing (b) regimes

When $k = 0$, $\mathrm{sn}\,(x, 0)$ is equal to $\sin(x)$ with $L = 2\pi$. As k approaches 1, $\mathrm{sn}\,(x, k)$ approaches $\tanh(x)$ and L approaches infinity.

The solution ψ is said to have *trivial phase* if $\theta(x)$ is constant and *nontrivial phase* if $\theta(x)$ is not constant. The nontrivial phase problem involves a large parameter space. In addition to the parameters α and β of the NLS equation (1), there are the admissible parameter choices of k and B to be considered. For simplicity, both NLS parameters are chosen to be ± 1, and the sign of the these parameters is used to classify the resulting equation. The NLS equation is said be *focusing* or *attractive* in the x-dimension if $\alpha > 0$. If $\alpha < 0$, NLS is said to be *defocusing* or *repulsive* in the x-dimension. Similarly, the sign of β will lead to focusing or defocusing in the y-dimension [13]. The NLS equation is called *hyperbolic* if $\alpha\beta < 0$ and *elliptic* if $\alpha\beta > 0$.

The phase contribution $\theta(x)$ of (4) implicitly depends on α and B in both (3) and (6). In order for both ϕ and θ to be real valued functions, we must chose $B \in [2k^2, 2]$ if $\alpha = 1$ or $B \leq 0$ if $\alpha = -1$. Figure 1 represents the (k, B) parameter space corresponding to nontrivial phase solutions of NLS. As the phase θ approaches zero, the nontrivial phase solutions should limit to one of the five possible types of trivial phase solutions; (*i*) Stokes wave, (*ii*) Jacobi elliptic cn, (*iii*) Jacobi elliptic dn, (*iv*) Jacobi elliptic sn, or (*v*) soliton type solutions. It is easily seen that the boundaries of the regions in figure (1) correspond to each of these trivial phase solutions. Table 2 summarizes the parameter values for which the NTP solutions reduce to trivial phase solutions.

While both trivial phase and nontrivial phase problems are of interest, trivial phase results are reasonably well represented in the literature; for example, see [14, 4, 2, 6, 8, 1, 12, 11], and much of this attention has been focused on soliton stability. The trivial phase limits will provide a reference for later discussion, when we refer to the stokes, sn, cn and dn trivial phase limits. The authors know of no published stability results in the nontrivial phase setting. (Is this true???). To begin to remedy this disparity, this paper numerically explores the linear stability of the nontrivial phase problem under transverse perturbation.

Table 1: Parameter values which reduce the nontrivial phase problem to the trivial phase problem.

Trivial phase	Non-trivial phase ($\alpha = -1$)	Non-trivial phase($\alpha = 1$)
Stokes	$k = 0, B \leq 0$	$k = 0, 0 \leq B \leq 2$
cn	N/A	$0 \leq k < 1, B = 2k^2$
dn	N/A	$0 \leq k < 1, B = 2$
sn	$0 \leq k < 1, B = 0$	N/A
soliton	Dark $k = 1, B = 0$ Grey $k = 1, B < 0$	Bright $k = 1, B = 2$

2 The linearized stability problem

In order to study the linear stability of nontrivial phase solutions of the NLS equation, we consider perturbations of the form

$$\psi_{_p}(x, y, t) = (\phi(x) + \epsilon u(x, y, t) + i\epsilon v(x, y, t))\mathrm{e}^{i\lambda t + i\theta(x)}, \tag{7}$$

where $u(x, y, t)$ and $v(x, y, t)$ are real-valued functions, ϵ is a small real parameter and $\phi(x)\mathrm{e}^{i\theta(x)+i\lambda t}$ is a nontrivial phase solution of the NLS equation. Substituting (7) into (1), linearizing and separating into real and imaginary parts leads to

$$\lambda u - 3\gamma\phi^2 u - \beta u_{yy} + \frac{1}{\phi^4}\alpha c^2 u - 2\alpha c\frac{1}{\phi^3}\phi_x v + 2\alpha c\frac{1}{\phi^2}v_x - \alpha u_{xx} = -v_t, \tag{8a}$$

$$\lambda v - \gamma\phi^2 v - \beta v_{yy} + \alpha c^2\frac{1}{\phi^4}v + 2\alpha c\frac{1}{\phi^3}\phi_x u - 2\alpha c\frac{1}{\phi^2}u_x - \alpha v_{xx} = u_t. \tag{8b}$$

at leading order.

Since (8) does not depend on y or t explicitly, we may assume that $u(x, y, t)$ and $v(x, y, t)$ have the forms

$$u(x, y, t) = U(x, \rho, \Omega)\mathrm{e}^{i\rho y + \Omega t} + c.c., \tag{9a}$$

$$v(x, y, t) = V(x, \rho, \Omega)\mathrm{e}^{i\rho y + \Omega t} + c.c., \tag{9b}$$

where ρ is a real constant, $U(x)$ and $V(x)$ are complex-valued functions, Ω is a complex constant and *c.c.* denotes complex conjugate.

If Ω has a positive real part, then the amplitudes of the perturbations grow exponentially in time and the unperturbed solution is said to be unstable. If the real part of Ω is negative, then the amplitudes of the perturbations decay in time and the unperturbed solution is said to be linearly asymptotically stable. If Ω is purely imaginary, then the perturbations oscillate in time and the unperturbed solution is said to be linearly (neutrally) stable. Upon substitution, (8) reduces to

$$\lambda U - 3\gamma\phi^2 U + \beta\rho^2 U + \alpha c^2\frac{1}{\phi^4}U - 2\alpha c\frac{1}{\phi^3}\phi_x V + 2\alpha c\frac{1}{\phi^2}V_x - \alpha U_{xx} = -\Omega V, \tag{10a}$$

$$\lambda V - \gamma\phi^2 V + \beta\rho^2 V + \alpha c^2\frac{1}{\phi^4}V + 2\alpha c\frac{1}{\phi^3}\phi_x U - 2\alpha c\frac{1}{\phi^2}U_x - \alpha V_{xx} = \Omega U. \tag{10b}$$

Written in operator form, (10) is

$$(L_1 + \beta\rho^2)U + SV = -\Omega V, \tag{11a}$$

$$(L_0 + \beta\rho^2)V - SU = \Omega U, \tag{11b}$$

where

$$L_1 = \lambda - 3\gamma\phi^2 + \alpha c^2 \frac{1}{\phi^4} - \alpha\partial_{xx}, \tag{12a}$$

$$L_0 = \lambda - \gamma\phi^2 + \alpha c^2 \frac{1}{\phi^4} - \alpha\partial_{xx}, \tag{12b}$$

$$S = -2\alpha c \frac{1}{\phi^3}\phi_x + 2\alpha c \frac{1}{\phi^2}\partial_x. \tag{12c}$$

If $c = 0$, then $S = 0$ in (11) and the problem reduces to the stability analysis of trivial phase solutions. This case is examined by Carter and Segur [2] and Carter and Deconinck in [6] and [1]. With the linear system (11) constructed, we are now able to consider stability of the perturbed nontrivial phase linearization via a numerical approach.

3 Stability

The spectrum of a linear problem is often computed using finite difference methods. Here, however, the size of the parameter space precludes the standard implementation of this technique. A spectral method due in essence to Hill is employed which uses periodicity of the coefficients to reduce the linear nontrivial phase stability problem to a family of spectral problems. For complete review of Hill's technique, which incorporates basic Floquet theory, see [3].

3.1 The numerical method

To apply Hill's method, Fourier expansions of L_1, L_0 and S, all of which are defined in (12), as well expansions of the unknown functions U and V are needed. The coefficients are written in the complex Fourier form as

$$\begin{aligned} \phi^2 &= \sum_{k=-\infty}^{\infty} Q_k e^{ik\pi x/L}, & \phi^{-2} &= \sum_{k=-\infty}^{\infty} R_k e^{ik\pi x/L}, \\ \phi^{-4} &= \sum_{k=-\infty}^{\infty} S_k e^{ik\pi x/L}, \quad \text{and} & \phi^{-3}\partial_x\phi &= \sum_{k=-\infty}^{\infty} T_k e^{ik\pi x/L}, \end{aligned} \tag{13}$$

where the values Q_k, R_k, S_k and T_k may be computed using a high-order quadrature scheme.

The periodicity of the coefficients containing powers of ϕ allows us to decompose the eigenfunctions of U and V of the spectral problem in a Fourier-Floquet form

$$U(x) := e^{i\mu x} \sum_{l=-\infty}^{\infty} U_l e^{-il\pi x/LP} \quad \text{and} \quad V(x) := e^{i\mu x} \sum_{l=-\infty}^{\infty} V_l e^{-il\pi x/LP}. \tag{14}$$

Here μ is a Floquet parameter and the factor of P is included for mathematical convenience. The form (14) results from an application of Floquet's theorem and then noting that we seek eigenfunctions, which are by definition bounded. Again, see [3] for a more complete explanation.

Substitution of (13) and (14) into (11) allows us to write equations for U_n and V_n as a coupled bi-infinite system of difference equations given by

$$-\left(\lambda+\beta\rho^2-\alpha\left(i\mu+\frac{in\pi}{LP}\right)^2\right)U_n+3\gamma\sum_{k=-\infty}^{\infty}Q_{\frac{n-k}{P}}U_k-\alpha c^2\sum_{k=-\infty}^{\infty}S_{\frac{n-k}{P}}U_k$$
$$+2\alpha c\sum_{k=-\infty}^{\infty}T_{\frac{n-k}{P}}V_k-2\alpha c\left(i\mu+\frac{in\pi}{LP}\right)\sum_{k=-\infty}^{\infty}R_{\frac{n-k}{P}}V_k=\Omega V_n \quad (15a)$$

$$\left(\lambda+\beta\rho^2-\alpha\left(i\mu+\frac{in\pi}{LP}\right)^2\right)V_n-\gamma\sum_{k=-\infty}^{\infty}Q_{\frac{n-k}{P}}V_k+\alpha c^2\sum_{k=-\infty}^{\infty}S_{\frac{n-k}{P}}V_k$$
$$+2\alpha c\sum_{k=-\infty}^{\infty}T_{\frac{n-k}{P}}U_k-2\alpha c\left(i\mu+\frac{in\pi}{LP}\right)\sum_{k=-\infty}^{\infty}R_{\frac{n-k}{P}}U_k=\Omega U_n, \quad (15b)$$

which hold for all n. Here $\mu\in[\frac{-\pi}{LP},\frac{\pi}{LP})$ and $Q_{\frac{n-k}{P}}=0$ if $\frac{n-k}{P}\notin\mathbb{Z}$.

In practice, a pre-multiplication of the linear system by ϕ^4 results in more rapid convergence of the Fourier coefficients. Also, an exact cosine series expansion of ϕ^2,ϕ^4 and ϕ^6 can be used, which follows from Jacobi's [7] series expansion of sn^2. This pre-multiplication transforms the original eigenvalue problem into a generalized eigenvalue problem. Golub and Van Loan [5] provide a brief discussion of generalized eigenvalue problems. For details of the numerical technique, see [9].

Notice that equations [15a-15a] are *equivalent* to the original system [12a-12b]. Only when truncated to a finite number of modes does this system become an approximation. If, for example, we take N to be maximimal mode number in the U_n and V_n approximations, then the exact coupled bi-infinite system reduces to a $(4N+2)$ system of equations.

3.2 Numerical experiments

Four cases were considered numerically:

- Defocusing in x with focusing perturbation in y. ($\alpha=-1$ and $\beta=1$)
- Defocusing in x with defocusing perturbation in y. ($\alpha=-1$ and $\beta=-1$)
- Focusing in x with focusing perturbation in y. ($\alpha=1$ and $\beta=1$)
- Focusing in x with defocusing perturbation in y. ($\alpha=1$ and $\beta=-1$)

In each case, a large number of parameter values were explored numerically. Approximately 5.2 million generalized eigenvalue problems were considered, the size of each determined by the cutoff mode of the underlying Fourier series. A truncation to N positive Fourier coefficients results in a $(4N+2)\times(4N+2)$ dimensional problem. The value of N as a function of (k,B) was chosen by computing sample problems over various k's and B's in the parameter region for increasingly large N until the eigenvalues that resulted stabilized qualitatively. A simple polynomial was then constructed to fit this data. This information, and details related to other parameter ranges

t

Table 2: Parameter values and ranges used in numerical experiments.

Parameter	Description	value
k	Elliptic Modulus	$\texttt{linspace(0,1,65)}$
B	Shift	For $\alpha=-1:$ $\quad -\texttt{logspace}(-8,0,65)$ For $\alpha=\ \ 1:$ $\quad (2k^2+\texttt{logspace}(-8,0,65))\cap(2k^2,2)$
N	Fourier cutoff	For $\alpha=-1:$ $\quad 15+\texttt{ceil}(5\texttt{k}^5)$ For $\alpha=\ \ 1:$ $\quad 10+\texttt{ceil}(25\texttt{k}^{10})$
ρ	perturbation wavenumber	$\texttt{linspace(0,4,65)}$
μ	Floquet parameter	$\texttt{linspace}(-\frac{\pi}{2\texttt{K}},\frac{\pi}{2\texttt{K}},21)$

used in the experiments, is given in Table 2. In the table, k is the elliptic modulus, B may be interpreted as a measure of nontrivial phase, N is the matrix dimension used to approximate the operators, ρ the wavenumber of the perturbation in the y-dimension, and μ the Floquet parameter. Also, $\texttt{linspace}(\texttt{a},\texttt{b},\texttt{m})$ is a linearly spaced vector from a to b of length m, $\texttt{logspace}(\texttt{a},\texttt{b},\texttt{m})$ is a logarithmically spaced vector from 10^a to 10^b of length m and $\texttt{ceil}$ is the ceiling function.

3.3 Numerical results

Using the Fourier-Floquet-Hill method we numerically considered the growth instabilities due to transverse perturbations with wavenumber denoted by ρ over the range of parameter values of table 2. Each numerical experiment consisted of computing the eigenvalues of a (generalized) eigenvalue problem. For each parameter triplet (k,B,ρ), for $\alpha,\beta=\pm1$, a sequence of Floquet parameters μ was chosen from the interval $[\frac{-\pi}{LP},\frac{\pi}{LP}]$. The eigenvalues and eigenvectors were computed from the resulting matrix. Although not included here, the corresponding eigenfunctions may be easily reconstituted from this information.

Since a single eigenvalue with positive real part will lead to instability of the system, the eigenvalue with largest real part over all choices of μ was recorded for each (k,B,ρ) triplet. That is, we compute

$$\Omega_{growth}(k,B,\rho)=\max_{\mu}(\Re(\Omega(k,B,\rho,\mu))),$$

which we call the growth rate. We reduce the dimension still further by computing the largest such instability over all sampled perturbation wave numbers ρ. This quantity,

$$\Omega_{\max}(k,B)=\max_{\rho}(\Omega_{growth}),$$

the maximal growth rate, is plotted in the first column of figure 3.3. We also recorded the minimum growth rate, which we computed as the minimum over ρ of Ω_{growth}. We plot the maximum over (k,B) of the maximal growth rate as well as the minimum over (k,B) of the minimal growth rate in the first column of plots. The second column indicates the wave number ρ which leads to maximal growth. The first two rows of the figure correspond the parameter range $(k,B)=(0,1)\times(2k^2,2)$ in the $\alpha=1$ case of 1(b), while the last two rows correspond to the x-defocusing parameter range of $(k,B)=(0,1)\times(-1,0)$.

Before we can discuss these plots, we need to describe the vertical axis used. For the first two rows, we transformed the quantity B via $T_f(B) = (B - 2k^2)/(2 - 2k^2)$. This maps the interval $[2k^2, 2]$ to $[0, 1]$. The transform for the last two rows was just $T_d(B) = -B$. In both cases, the result of the transform is to scale the B interval to [0,1]. In all cases we present the plots using a $\log_{10}$ scale of the vertical dimension.

In the case of $\alpha = 1$, the growth plots clearly indicate that system stability changes dramatically as B moves away from the cn trivial phase limiting case, which approached at the bottom of the each respective plot, towards the dn trivial phase limiting case, located at the top edge of these plots. This same rapid growth feature is evident in the case where $\alpha = -1$, as seen in 3(a) and 4(a). In these plots, the lower limit of the plot corresponds to $B = -1e - 8$, and so is just slightly away from the sn trivial phase limit case. This suggests that small changes in c, which is a scaling quantity for the nontrivial phase term $\theta(x)$, leads to large changes in the physical behavior.

The sign of α appears to be a important factor that can be used to distinguish the stability surfaces. When $\alpha = 1$, the largest instability is achieved for relatively large values of k, in contrast the location of the max growth of $\alpha = -1$, which occurs for relatively small values of k, near the stokes trivial phase limiting case. Also, the distinct local nature of the maxima in the $\alpha = 1$ cases is different from the more global nature of the maxima in the $\alpha = -1$ setting. The overall qualitative structure of the growth surface is quite similar in both the focusing case (figures 1-2(a)) and in the defocusing case (figures 3-4(a)). The position of both the maxima and minima appear to be influenced only slightly by the sign of the perturbation, both for $\alpha = 1$ and when $\alpha = -1$. In all cases, the minimum growth rate is found nearest to the stokes limit of $k = 0$. It is interesting to note is that the stability factor does not grow monotonically for any choice of $k \in (0, 1)$. Instead, the maximal growth rate is achieved at some point in the interior of the admissible parameter space.

The wavenumber of the perturbation leading to largest growth is plotted in column (b) of figure (3.3). The case of $\alpha = -1$ and $\beta = -1$, the long wave $\rho = 0$ perturbation results in the largest growth. In all other cases, it is the short wave length instabilities (large ρ) that lead to the largest growth. For $\alpha = 1$ $\beta = 1$, the max instability occurs for the shortest wavelength samples, although there appears to be a possible periodicity in the region where k is larger than about 0.95. In fact, there appears to be periodicity in several subregions in these plots, most clearly seen in the horizontal banding in the upper the section of plot 2(b) of 3.3 and in the vertical banding at the bottom and in the left of this same plot. The growth factor appears constant, but the corresponding wave number appears to sweep through a distinct range of ρ values.

3.4 Perturbation approach

Generalizing the work of cite? who to site here? in the soliton setting, we construct perturbations to explore the stability of the nontrivial phase solutions in the large ρ limit. For large ρ, we consider series of the form

$$U(x) \sim u_0(\eta x) + \rho^{-1} u_1(\eta x) + \rho^{-2} u_2(\eta x) + \dots \tag{16a}$$

$$V(x) \sim v_0(\eta x) + \rho^{-1} v_1(\eta x) + \rho^{-2} v_2(\eta x) + \dots \tag{16b}$$

$$\Omega \sim \omega_{-2}\rho^2 + \omega_{-1}\rho + \dots \tag{16c}$$

$$\eta \sim \eta_{-1}\rho + \eta_0 \tag{16d}$$

where u_j and v_j are complex valued functions, ω_j is a complex constant, and η_j is a real constant.

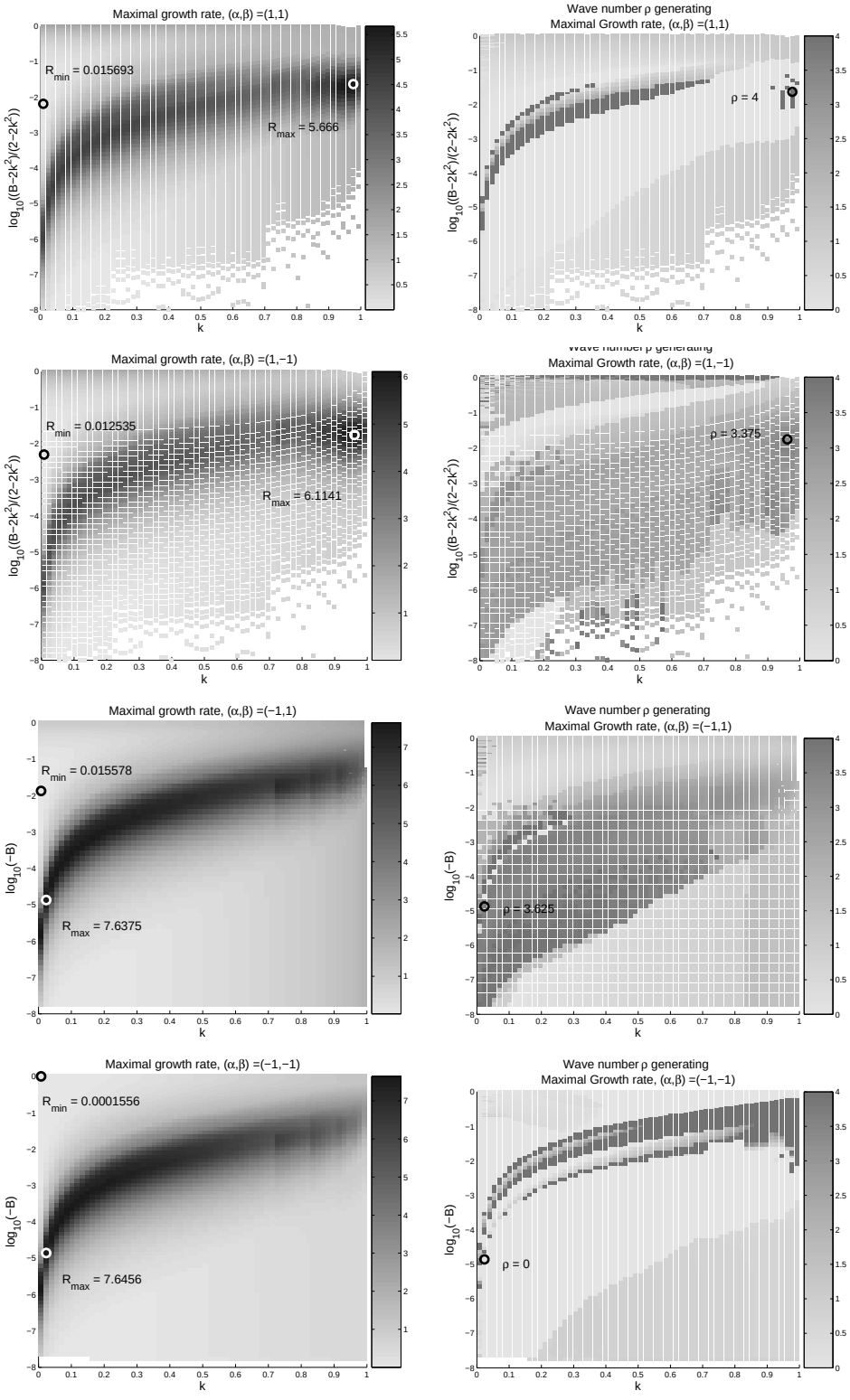

1

2

3

4

(a) (b)

Figure 2: Plots representing (a) maximum spectral growth for $\rho \in [0, 4]$ and (b) indicating corresponding wave number leading to instability. Here $R_{\max} = \max_{k,B,\rho}(\max_{\mu}(\Re(\Omega)))$ and $R_{\min} = \min_{k,B,\rho}(\max_{\mu}(\Re(\Omega)))$. The vertical axis is on a $\log_{10}$ scale.

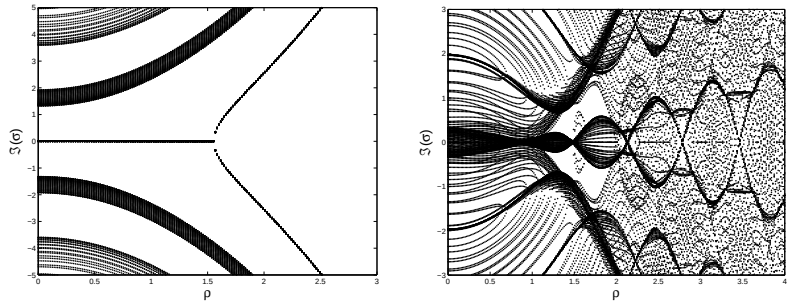

(a) (b)

Figure 3: Projection of spectrum onto the $(\rho, \Im(\Omega))$ plane for (a) $\alpha\beta > 0$ and (b) $\alpha\beta < 0$.

I could include all or part of this :

Substituting into the linear problem generates

$$\alpha\eta_{-1}^2 u_0'' - \beta u_0 - \omega_{-2} v_0 = 0 \tag{17a}$$

$$\alpha\eta_{-1}^2 v_0'' - \beta v_0 + \omega_{-2} u_0 = 0 \tag{17b}$$

at leading order. Transforming to a first order system generates

$$\begin{pmatrix} u_0 \\ u_0' \\ v_0 \\ v_0' \end{pmatrix}' = \begin{pmatrix} 0 & 1 & 0 & 0 \\ \frac{\beta}{\alpha\eta_{-1}^2} & 0 & \frac{\omega_{-2}}{\alpha\eta_1^2} & 0 \\ 0 & 0 & 0 & 1 \\ \frac{\omega_{-2}}{\alpha\eta_{-1}^2} & 0 & \frac{\beta}{\alpha\eta_1^2} & 0 \end{pmatrix} \begin{pmatrix} u_0 \\ u_0' \\ v_0 \\ v_0' \end{pmatrix}. \tag{18}$$

The eigenvalues λ of (18) satisfy

$$\left(\lambda^2 - \frac{1}{\alpha\eta_{-1}^2}(\beta + i\omega_{-2})\right)\left(\lambda^2 - \frac{1}{\alpha\eta_{-1}^2}(\beta - i\omega_{-2})\right) = 0. \tag{19}$$

If the real part of ω_{-2} is non-zero, then $\Re(\lambda)$ will also be non-zero. We seek bounded solutions, and so assume that ω_{-2} is purely imaginary. Since it is easier to first find all unbounded solutions and then exclude them, we do so. By requiring

$$\frac{1}{\alpha}(\beta + i\omega_{-2}) > 0 \quad \textbf{AND} \quad \frac{1}{\alpha}(\beta - i\omega_{-2}) < 0$$

a parameter space corresponding to unbounded solutions may be found. If $\frac{\beta}{\alpha} > 0$ then there are no bounded eigenfunctions if $-\beta < i\omega_{-2} < \beta$. Since $\Omega \sim \omega_{-2}\rho^2$, we conclude that there will be no eigenvalues (at first order) of the form (16c) with non-zero real part in the region between ρ^2 and $-\rho^2$. If $\frac{\beta}{\alpha} < 0$ then we need to satisfy $\beta > i\omega_{-2}$ and $\beta < -i\omega_{-2}$, which is impossible. As a consequence, the spectrum will will apparently occupy the full complex sheet.

I stopped here.
or just the summary:

3.4.1 Perturbation results

These assumptions can be shown to imply that, arguing first order contributions , the cases in which $\alpha\beta > 0$ should have a spectrum whose imaginary part must not lie in the region bounded between ρ^2 and $-\rho^2$ in the $(\rho, \Im(\Omega))$ plane. Continuing the analysis to second order leads to the conclusion that $\omega_{-1} = 0$. In the case where $\alpha\beta < 0$, it is possible to show that no region of unbounded growth may be excluded by the assumptions. This suggests that the projection onto the spectrum onto the $(\rho, \Im(\Omega))$ plane will appear full. These claims are supported by the plots of figure (3.4), which are qualitatively similar to the plots for all admissible choices of k and B.

4 Conclusions

The linear stability of nontrivial phase solutions to the cubic Nonlinear Schrödinger equation was explored. A numerical method was used to generate eigenvalue information over a wide range of parameter values. Plots were presented that reported growth factors and wave-numbers resulting in maximal instability. A rapid increase in the rate of instability resulted from the addition of nontrivial phase $\theta(x)$. A movement through the shifted B space indicated that values which correspond to the largest growth factors occur in the parameter region which corresponds to fully nontrivial solutions. In summary, numerical evidence suggests that bounded, nontrivial one dimensional solutions to the cubic NLS equation are unstable in the presence of transverse perturbation.

References

[1] J. Carter and B. Deconinck. Stability of trivial phase solutions fo the two-dimensional cubic nonlinear schrödinger equation. *in preparation*, 2005.

[2] J. Carter and H. Segur. Instability in the two-dimensional cubic nonlinear schrödinger equation. *Phys. Rev. E.*, 68(4):#045601, 2003.

[3] B. Deconinck and J. N. Kutz. Computing spectra of linear operators using Hill's method. *in preparation*, 2005.

[4] A.M. Rubenchik E.A. Kuznetsov and V.E. Zakharov. Soliton stability in plasmas and hydrodynamics. *Phys. Rep.*, 142:103–165, 1986.

[5] G. H. Golub and C. F. Van Loan. *Matrix Computations*. Johns Hopkins University Press, 1996.

[6] B. Deconinck J. Carter and D. E. Pelinovsky. Transverse instabilities of deep-water solitary waves. *in preparation*, 2005.

[7] C. G. Jacobi. *Fundamenta Nova Theoriae Functionum Ellipticarum*. Königberg, 1829.

[8] Y. S. Kivshar and D. E. Pelinovsky. Self-focusing and transverse instabilities of solitary waves. *Phys Rep*, 331(4):118–195, 2000.

[9] C. Moler and G.W. Stewert. An algorithm for generalized matrix eigenvalue problem. *SIAM J. Numer. Anal.*, 10(2), 1973.

[10] K. Rypdal and J. J. Rasmussen. Blow-up in nonlinear schrödinger equations. i. a general review. *Physica Scripta*, 33:481–497, 1986.

[11] G. M. Fraiman S. E. Fil'chenkov and A. D. Yunakovskii. Instability of periodic solutions of the nonlinear schrödinger equation. *Sov. J. Plasma Phys.*, 18(8):961–966, 1987.

[12] P. L. Sulem and C. Sulem. *Nonlinear Schrödinger Equations: Self-focusing and Wave Collapse*. Springer-Verlag, NY, 1999.

[13] V. E. Zakharov and A. M. Rubenchik. ??? *Sov Phys JETP*, 38(3):494, 1974.